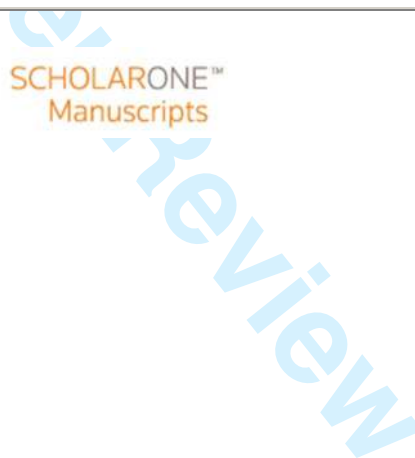


**Spatial aggregation of time variant stream water ages in urbanizing catchments**

Journal:	<i>Hydrological Processes</i>
Manuscript ID:	HYP-14-0990.R1
Wiley - Manuscript type:	Scientific Briefing
Date Submitted by the Author:	21-Mar-2015
Complete List of Authors:	Soulsby, Chris; University of Aberdeen, School of Geosciences Birkel, Christian; University of Costa Rica, Department of Geography Geris, Josie; University of Aberdeen, School of Geosciences Tetzlaff, Doerthe; University of Aberdeen, School of Geosciences
Keywords:	isotopes, transit times, conceptual models, non-stationarity, urban hydrology



# Spatial aggregation of time variant stream water ages in urbanizing catchments

C. Soulsby<sup>1</sup>, C. Birkel<sup>1,2</sup>, J. Geris<sup>1</sup> and D. Tetzlaff<sup>1</sup>

<sup>1</sup>School of Geosciences, University of Aberdeen, Aberdeen, AB24 3UF.

<sup>2</sup>Department of Geography, University of Costa Rica, 2060 San José, Costa Rica.

## ABSTRACT

We calibrated an integrated flow-tracer model to simulate spatially distributed isotope time series in stream water in a 7.9 km<sup>2</sup> catchment with an urban area of 13%. The model used flux tracking to estimate the time-varying age of stream water at the outlet and both urbanised (1.7 km<sup>2</sup>) and non-urban (4.5 km<sup>2</sup>) sub-catchments over a 2.5 year period. This included extended wet and dry spells where precipitation equated to >10 year return periods. Modelling indicated that stream water draining the most urbanised tributary was youngest with a Mean Transit Time (MTT) of 171 days compared with 456 days in the non-urban tributary. For the larger catchment the MTT was 280 days. Here, the response of urban contributing areas dominated smaller and more moderate runoff events, but rural contributions dominated during the wettest periods, giving a bimodal distribution of water ages. Whilst the approach needs refining for sub-daily time steps, it provides a basis for projecting the effects of urbanisation on stream water transit times and their spatial aggregation. This offers a novel approach for understanding the cumulative impacts of urbanisation on stream water quantity and quality which can contribute to more sustainable management.

**Keywords:** isotopes, transit times, conceptual models, non-stationarity, urban hydrology

## 1. INTRODUCTION

Advances in quantifying the travel times of water through catchments have shown that this depends on the interaction of flow path partitioning, the size and nature of the soil and groundwater stores

1  
2  
3 25 and the associated mixing processes that assimilate precipitation into storage (McDonnell et al.,  
4  
5 26 2010). An important insight has been awareness of time variant influences on transit time  
6  
7 27 distributions (TTDs) as highlighted by Rodhe et al. (1996). This time variance reflects the role of  
8  
9 28 short-term individual storm event characteristics and antecedent conditions (Birkel et al., 2012); the  
10  
11 29 effects of seasonal and inter-annual climatic variability (Hrachowitz et al., 2013; Heidbuechel et al.,  
12  
13 30 2013), the mixing assumptions for different stores (Fenicia et al., 2010; van der Velde et al., 2014)  
14  
15 31 and the impact of extreme events (Lyon et al., 2008). Sensitivity of catchment TTDs thus varies  
16  
17 32 geographically depending upon catchment characteristics and the variation in hydroclimate (Tetzlaff  
18  
19 33 et al., 2009). Full understanding is predicated on long-term data sets characterizing climatic variability  
20  
21 34 (Hrachowitz et al., 2009), high resolution tracer sampling to capture short-term dynamics (Roa-  
22  
23 35 Garcia and Weiler, 2010), characterisation of older waters (Stewart et al., 2010) and identification of  
24  
25 36 ecohydrologically relevant mixing of waters and solutes (Brooks et al., 2009). Only then can the  
26  
27 37 response of catchments be tracked as it transits through dry periods and times of extreme wetness.  
28  
29  
30  
31  
32

33  
34  
35 39 More sophisticated modelling approaches are also needed to capture time variant processes that  
36  
37 40 govern the routing of water and solutes. These should ideally go beyond traditional lumped, time-  
38  
39 41 invariant convolution approaches to fitting TTDs to input-output data. Recent developments include  
40  
41 42 more robust theoretical frameworks for modelling the temporal dynamics of water and solute  
42  
43 43 transport (Botter et al., 2011; Duffy, 2010; Heidbuechel et al., 2012; Rinaldo et al., 2011), use of  
44  
45 44 conceptual rainfall-runoff models to track tracer fluxes and water ages (Dunn et al., 2010; McGuire  
46  
47 45 et al., 2007; Hrachowitz et al., 2013) and the use of particle tracking to simulate evolution of stream  
48  
49 46 water transit time distributions (Davies et al., 2013). Such models should – ideally – have minimum  
50  
51 47 parameterisation to improve identifiability and reduce uncertainty (Beven, 2012). In this regard  
52  
53 48 using both flow and tracers metrics in combined objective functions allows to constrain model  
54  
55 49 structures, improve calibration and aid model evaluation (Birkel et al., 2014).  
56  
57  
58  
59  
60

50

51 Such coupled flow-tracer models can provide a step forward for using time variant transit time  
52 analysis in applied hydrology. McDonnell and Beven (2014) identified consistent conceptualisation of  
53 hydrological response celerity with pore water **velocities** distributions as a major research frontier in  
54 hydrology. Progress is needed to produce models that can adequately characterise the hydrological  
55 response dynamics, storage characteristics and mixing relationships in catchments. Only then can  
56 robust projections be made about how catchments mediate impacts of land use change on stream  
57 water quantity and quality in terms of routing, storage dynamics and transit times (Gall et al., 2013).  
58 Monitoring effects of land use change on tracer dynamics, thus, provides an opportunity for testing  
59 such integrated modelling approaches. It also provides an experimental framework for testing  
60 hypotheses about how flow partitioning, storage dynamics and water transit times change.  
61 Urbanisation provides rapid, direct and large-scale hydrological impacts that affect extensive parts of  
62 the world (Grimm et al., 2008). This has policy relevance as more sustainable approaches to urban  
63 planning seek to retain catchment storage functions by minimising the extent of impermeable  
64 surfaces and creating retention wetlands to mitigate increased flood risk, reduced summer low flows  
65 and deterioration of water quality (e.g. Niemczynowicz, 1999; Zipperer et al., 2000). This can be  
66 assisted by understanding how the urban environment affects transit times.

67

68 Here we use spatially distributed tracer data from an urbanising catchment which transitioned  
69 through some hydroclimatic extremes over a 2.5 year period. These are used together with a  
70 coupled flow-tracer model to answer the following questions: (1) What are the time-variant  
71 characteristics of the age composition of stream water draining urban and non-urban environments?  
72 (2) How is the time-variance of stream water age composed in relation to the influence of different  
73 land uses at larger scales? (3) Can we use such models to predict the impact of urbanisation on the

1  
2  
3 74 stream water age? We also highlight research needs for such work to inform the development of  
4  
5 75 green infra-structure to facilitate more sustainable approaches to managing urban water.  
6  
7

8 76  
9

## 10 77 **2. STUDY AREA AND DATA**

11  
12  
13  
14 78 The study site is the Burn of Bennie, a 7.9km<sup>2</sup> catchment (Fig. 1 and Table 1) in NE Scotland. Two  
15  
16 79 tributaries with similar soils, geology and topography, form the headwaters; one rural in the north  
17  
18 80 has ~1% urban influence and drains a patch work of forest, wetland and farmland. The southern  
19  
20 81 tributary has been subject to increased urbanisation over the past two decades (now covering 12.4%  
21  
22 82 of its area), with the lower catchment downstream of the main tributary confluence being similarly  
23  
24 83 impacted (13.1% total). Further urban expansion is planned around the southern tributary,  
25  
26 84 increasing the total urbanised area of the catchment to 16.3%  
27  
28 85 (<http://aberdeenshire.gov.uk/statistics/area/BanchoryProfile2013.pdf>). The climate is temperate;  
29  
30 86 mean annual precipitation is 950mm (varying between ~700-1000mm), mean July and December  
31  
32 87 temperatures are 13°C and 7°C, respectively. Potential evapotranspiration is 500mm and fairly  
33  
34 88 constant. The catchment is underlain by a uniform, low permeability bedrock covered by deep (10-  
35  
36 89 20m) layers of glacial drift, with alluvium in the river valleys. The drifts are coarse textured and  
37  
38 90 podzolic soils, which are mainly freely-draining, dominate.  
39  
40  
41  
42  
43  
44  
45

46 92 Five sites were sampled from October 2011 at approximately weekly intervals (Fig. 1 and Table 1).  
47  
48 93 These include the main catchment outfall (ID=outlet), and the lowest points on the rural (ID=rural)  
49  
50 94 and urban tributaries (ID=urban). Also, a site on the upper urban tributary was sampled (ID=urban a)  
51  
52 95 as was the outflow from a retention pond draining a recently urbanised area (ID=urban b). Sampling  
53  
54 96 targeted hydrological events; most significant events were sampled and larger events were sampled  
55  
56 97 daily over the hydrograph. Daily precipitation samples were collected from a small weather station  
57  
58  
59  
60

1  
2  
3 98 (Fig. 1). Samples were analysed at the University of Aberdeen for  $^{18}\text{O}$  and  $^2\text{H}$  using a Los Gatos DLT-  
4  
5 99 100 (2nd generation) laser spectrometer and are reported in  $\delta$  units (‰) relative to Vienna Standard  
6  
7 100 Mean Ocean Water (V-SMOW). Analytical precision was 0.2‰ for  $\delta^{18}\text{O}$  and 0.4‰ for  $\delta^2\text{H}$ . Given the  
8  
9 101 greater relative precision we use  $\delta^2\text{H}$  in the modelling that follows.  
10  
11

12  
13  
14  
15  
16  
17  
18  
19  
20  
21  
22  
23  
24  
25  
26  
27  
28  
29  
30  
31  
32  
33  
34  
35  
36  
37  
38  
39  
40  
41  
42  
43  
44  
45  
46  
47  
48  
49  
50  
51  
52  
53  
54  
55  
56  
57  
58  
59  
60

102  
103 Precipitation data from 14 surrounding daily gauges were used from the MIDAS data sets at the  
104 British Atmospheric Data Centre to derive daily areal totals via spatial interpolation with the gradient  
105 inverse distance method (Stahl *et al.*, 2006) on a 100m grid. An Automatic Weather Station 10km  
106 south of the site was used to derive ET estimates for the catchment using Penman-Monteith. Due to  
107 vandalism problems, continuous flow gauging in the urban catchment was precluded. Thus, we used  
108 the method of Seibert and Beven (2009) to manually gauge flows (10 gaugings in total) across the  
109 flow spectrum as calibration targets for a runoff model to produce flow time series. This was found  
110 to give acceptable estimates of daily flows at the rural, urban and outlet sites (see Soulsby *et al.*,  
111 2014).  
112

### 113 3. INTEGRATED FLOW-TRACER MODEL

#### 114 3.1 Model structure

115 We used the data to develop a simple conceptual, tracer-aided rainfall-runoff model representing  
116 the two main landscape units (urban and rural) combined in three sub-catchments represented by  
117 the rural, urban and outlet sites (Figure 2). After testing different arrangements of the stores in the  
118 model we settled on the most parsimonious semi-distributed structure. This consisted of a single  
119 linear reservoir draining urban areas (storage component  $S_{urban}$  drained by the rate parameter  $u$ ) and  
120 a two-reservoir model for rural areas. The upper reservoir  $S_{up}$  was parameterised (rate parameters  $k$   
121 and nonlinearity parameter  $\alpha$ ) with a nonlinear power-function type equation to account for faster

1  
2  
3 122 flow components. The lower reservoir  $S_{low}$  is filled by a linear recharge flux (parameter  $r$ ) and linearly  
4  
5 123 contributes to streamflow via the rate parameter  $b$ . Both components add up to total stream flow.  
6  
7 124 For mixed landscape sub-catchments, the rural and urban model units were combined, with the  
8  
9 125 areal fraction of their flow-tracer contribution to the catchment outlet summing to one.  
10  
11

12  
13 126

14  
15 127 Tracer transport and mixing was directly linked to the hydrological reservoirs using a mixing cell  
16  
17 128 approach similar to Hrachowitz et al. (2013):  
18

19  
20  
21 129 
$$\frac{d(c S)}{dt} = \sum_j c_{I,j} I_j - \sum_k c_{O,k} O_k$$
 Eq. 1  
22  
23

24  
25 130 With  $c$  being the isotope signature of storage components (‰) in  $j$  storage inflows  $I_j$  (precipitation  
26  
27 131 and recharge) and  $k$  outflow  $O_k$  components (actual evapotranspiration  $ET_{act}$  and upper reservoir  
28  
29 132 outflow  $Q_{up}$ ), which characterizes the catchment storage  $S$  dynamics (sum of dynamic and additional  
30  
31 133 storage components available for mixing that do not affect the water fluxes) and associated isotope  
32  
33 134 signature  $c$ . Additional mixing stores were calibration parameters in the form of fixed mixing  
34  
35 135 volumes ( $MV_{up}$  in  $S_{up}$  and  $MV_{low}$  in  $S_{low}$ ). These facilitate reproduction of observed tracer attenuation  
36  
37 136 in streams. As urban reservoirs are assumed to directly contribute tracers to the stream no mixing  
38  
39 137 parameters were used. We did not incorporate isotopic fractionation as tests did not show an  
40  
41 138 improvement to simulations. For the different subcatchments, the same parameters were applied to  
42  
43 139 represent the same landscape units and keep the model as parsimonious as possible (7 parameters  
44  
45 140 in total; 5 rainfall-runoff and 2 tracer parameters as indicated in Fig. 2).  
46  
47  
48  
49

50 141 **3.2 Water age estimates**  
51

52  
53 142 We used a flux tracking approach (Hrachowitz *et al.*, 2013) to estimate water age. As each new daily  
54  
55 143 input flux can be labelled, the evolving age of water in different stores can be tracked to give a final  
56  
57 144 age label upon discharge to the stream. The stream water age is then calculated as a flux-weighted  
58  
59  
60

1  
2  
3 145 age from the contributions of the urban and upper and lower reservoirs. Time variant water age  
4  
5 146 distributions for flow generated from the different units and sub-catchments ~~was~~ then calculated:  
6  
7

$$147 \quad p_{F,Q}(t_j - t_i, t_j) = \sum_{n=1}^N p_{F,Q_n}(t_j - t_i, t_j) \frac{Q_n(t_j)}{Q(t_j)} \quad \text{Eq. 2}$$

8  
9  
10  
11  
12  
13 148 ~~Where~~  $p_{F,Q}$  is the distribution of water age of contributing fluxes  $Q_n$  to total discharge  $Q$  with  $t_j$  being  
14  
15 149 the time of exit at the catchment outlet and  $t_i$  the time of entry with precipitation. Simulations used  
16  
17 150 a 5 year warm-up period to initialise storage filling, signatures and water ages (starting at 1 with the  
18  
19 151 first day of simulations). Isotope storage values were initially set to observed mean discharge  
20  
21 152 signatures for each site. Actual planning proposals for new urban areas (Fig. 1) were used to predict  
22  
23 153 impacts on water age distributions using the calibrated model, assuming a stationary climate.  
24  
25  
26  
27  
28  
29

### 30 155 3.3 Model calibration

31  
32  
33 156 We integrated calibration objectives using the manual point gaugings for the streamflow targets and  
34  
35 157 isotope time series measured at the urban, rural, and outlet sub-catchments as the tracer targets.  
36  
37 158 We also used the ratio of measured flows of the rural and urban sub-catchments as an additional  
38  
39 159 stream flow target. Calibration used the modified Kling-Gupta efficiency (KGE) for the two separate  
40  
41 160 (streamflow  $KGE\_Q$  and tracer  $KGE\_D$ ) objectives (Kling *et al.*, 2012):  
42  
43  
44

$$161 \quad KGE = 1 - \sqrt{(1-r)^2 + (1-\gamma)^2 + (1-\beta)^2} \quad \text{Eq. 3}$$

45  
46  
47  
48 162 The  $KGE$  is a three-dimensional representation (Euclidean distance) of the widely-used Nash-  
49  
50 163 Sutcliffe criterion balancing dynamics (correlation coefficient  $r$ ), bias (bias ratio  $\beta$ ) and variability  
51  
52 164 (variability ratio  $\gamma$ ) with a perfect fit of 1. The combined streamflow and tracer targets were equally  
53  
54 165 weighted and minimized as the unknown Euclidean distance from the optimal model using a multi-  
55  
56 166 objective Non-dominated Sorting Genetic evolution Algorithm (NSGA) (Deb *et al.*, 2002). This  
57  
58  
59  
60



1  
2  
3 167 searches a relatively wide initial parameter space and sequentially combines and updates 500  
4  
5 168 parameter sets over 1000000 iterations until no further improvement can be established. The best  
6  
7 169 500 parameter sets were used for subsequent analysis.  
8  
9

10  
11 170

### 12 13 171 **3.4 Parameter identifiability**

14  
15  
16 172 We used a regional sensitivity analysis (RSA) (Hornberger and Spear, 1981) to assess identifiability of  
17  
18 173 the best 500 parameter sets. The resulting curves or constrained parameter spaces indicate  
19  
20 174 identifiability, while a straight line over the initial parameter space shows non-identifiability.  
21  
22

23  
24 175

### 25 26 176 **3.5 Lumped convolution integral model**

27  
28  
29 177 Transit times from the flow-tracer model were compared to a time invariant convolution integral  
30  
31 178 model (see Hrachowitz et al., 2009) using the two-parameter (shape parameter  $\alpha$  and scale  
32  
33 179 parameter  $\beta$ ) gamma distribution as a transfer function (Kirchner et al., 2001). The KGE criterion was  
34  
35 180 used to calibrate the gamma model (GM) with a single target (isotope time series measured for each  
36  
37 181 sub-catchment) using a simple Differential Evolution (DE) algorithm for optimization (Mullen *et al.*,  
38  
39 182 2010). The 2.5 yr record was used for calibration with a warm-up of 5 years. Due to the insensitivity  
40  
41 183 of stable isotopes in detecting older water, the  $\beta$  parameter was set to the upper limit of 5 years.  
42  
43  
44

45  
46 184

## 47 48 185 **4. RESULTS**

### 49 50 186 **4.1 Hydroclimatic and isotopic variability**

51  
52  
53  
54 187 During the study the site experienced a range of unusual and contrasting hydroclimatic extremes  
55  
56 188 (Fig. 3). The first year had a dry winter, but the summer of 2012 was the wettest for 20 years in NE  
57  
58  
59  
60

1  
2  
3 189 Scotland. In the second year, the autumn was wet and in Dec. 2012 the highest daily precipitation  
4  
5 190 totals and flows were recorded. This was followed by a warm dry summer in 2013 corresponding to  
6  
7 191 a 10 year return period drought which persisted through autumn but was followed by high  
8  
9 192 precipitation in both Jan. and Feb. 2014 (see UK Hydrological Summaries for individual months at  
10  
11 193 <http://www.ceh.ac.uk/data/nrfa>).

13  
14  
15 194

16  
17 195 Isotopes in precipitation exhibited general seasonal differences between winter depletion and  
18  
19 196 summer enrichment, but day-to-day variability within season was marked (Fig. 3). Isotope variability  
20  
21 197 in stream flow was most pronounced in the most urbanised sites (Table 2), with urban impacts  
22  
23 198 evident in rapid, direct routing of tracer signals in precipitation both in small and large events.  
24  
25 199 Variations were attenuated in the rural tributary where dynamics in stream water isotope signals  
26  
27 200 were exhibited more gradual changes in the wetter periods in June and Dec. 2012 and Jan/Feb 2013.  
28  
29 201 At sites with both rural and urban influence, the tracer variations reflect both the urban influence of  
30  
31 202 marked isotopic variability in smaller events but a general damping in large events and baseflows.  
32  
33

34  
35  
36 203

#### 37 38 204 **4.2 Flow-tracer model simulation results**

39  
40  
41 205 The integrated flow-tracer model captured the measured peak discharge and following recession  
42  
43 206 period in Dec. 2012 (Figure 4a). Additionally, the model was able to match the observed lower flows,  
44  
45 207 despite failing to reproduce the higher observed flows in June 2012. However, the model did capture  
46  
47 208 small and moderate events with dry antecedent conditions where the lower catchment response is  
48  
49 209 dominated by the urban response. The model calibrated to the common flow target performed  
50  
51 210 reasonably well with a best-fit KGE = 0.66 ( $R^2 = 0.72$ ). Also, most rainfall-runoff model parameters  
52  
53 211 were identifiable over a constrained range (Fig. 5 and Table 3). The least constrained were the  
54  
55 212 nonlinearity parameter  $\alpha$  and the recharge rate parameter  $r$ .  
56  
57  
58  
59  
60

213

214 Stream isotope variations were captured quite well and the posterior variability of the best 500  
215 parameter sets bracket most of the observations (Fig. 4b-d). Additional mixing volumes were  
216 identifiable with a constrained upper volume  $MV_{up}$  (150 to 280mm) and an identifiable parameter  
217 region of  $MV_{low}$  at  $> 800$ mm (Fig. 5e and f). The best isotope simulations were for the most  
218 urbanised catchment; best-fit KGE of 0.86 and  $R^2$  of 0.89 (Fig. 4d). In the rural tributary the challenge  
219 of the damping was exacerbated by the effects of evaporative fractionation in the summer of 2014  
220 (Fig. 4c). Thus, invariant isotope values were simulated in outflows from the lower groundwater box  
221 which also failed to capture short-term effects of summer events or fractionation. This also  
222 explained why isotopic fractionation tests showed little model improvement. Nevertheless, overall  
223 simulations were reasonable (best-fit KGE = 0.78 and  $R^2 = 0.8$ ). The summer problems were also  
224 evident to a lesser extent in the simulations for the integrated lower catchment, where the lowest  
225 flows are generally dominated volumetrically by the rural catchment (Fig. 4d and Table 3). However,  
226 again, overall the model performed well over the whole period (best-fit KGE = 0.83 and  $R^2 = 0.85$ ).

227

### 228 **4.3 Spatial aggregation on stream water age estimates**

229 Stream water ages were estimated by aggregating the age of water derived from flux tracking in the  
230 different model landscape units, revealing marked differences for the 3 sites (Fig. 6). In the rural  
231 tributary ages show a bimodal distribution (Fig. 6c and c1); with a 50-100 day peak for larger events,  
232 and a secondary peak of 350-400 days reflecting the heavy tailing of old water contributions at base  
233 flow. The influence of such slower, deeper flow paths is emphasised by  $<50\%$  of tracer recovery  
234 being modelled at the end of a year. In contrast, the outflow of the modelled urban response unit  
235 indicated the very short residence times; here, most stream water is a few days old, and about 70%  
236 of the flux occurred in  $<50$  days, with  $>95\%$  tracer recovery within 400 days (Fig. 6a and a1). In mixed

237 land use catchments (urban and outlet), the integration of both sources are evident (Fig. 6b and c).

238 In the urban tributary, the distribution is modal in the 50-100 day age class, with limited tailing (Fig.

239 6b and b1). However, at the lower site (outlet) the distribution is bi-modal with the urban area giving

240 50-100 day modal class, and rural inputs causing a secondary peak at 300-400 days (Fig. 6d and d).

241

242 The Transit Time Distribution derived using the time invariant Gamma Model fitted to the input-

243 output data had lower performance statistics than the flow-tracer model though still reasonable fits

244 (Table 4). The  $\alpha$  parameter in the GM was 0.63 for the rural site, but reduced to 0.2 as the

245 percentage urban area increased. Such a decrease with increasing urban cover was also observed for

246 the MTT. The beta parameter was not identifiable and remained close to the upper boundary of 5

247 years. The derived best-fit MTTs for the urban, rural and outlet sites from the GM at 366, to 1050 to

248 456 days respectively, were shorter than for the flux tracking. However, the posterior variability

249 (indicated by the best 500 parameter sets) of the flow-tracer model indicates significant uncertainty

250 (Table 4) which generally brackets the GM estimates.

251

#### 252 4.4 Future urban development

253 The model was also used for projecting future change by increasing the urban area based on actual

254 planning proposals (Fig. 1). Resulting changes to the cumulative frequency distributions of median

255 water ages shows accelerated routing of water and reduced storage at both the urban and outlet

256 sites, with consequent reduced water ages (Fig. 7). The rural tributary remains unchanged. The

257 uncertainties of the projections are large and overlap as indicated in Table 4, but the direction of

258 change is evident in the median age distributions and consistent with impacts so far. Thus, even if

259 relatively small parts of a catchment are affected by urbanization, this is still sufficient for a dramatic

260 effect on TTDs that can propagate to the larger catchment scale. Although the rural tributary

1  
2  
3 261 remained unchanged, just a 3% increase in urban area showed a clear impact with the future outlet  
4  
5 262 median age CDF approximating the current urban site.  
6  
7

8 263  
9

## 10 264 **5. DISCUSSION**

### 11 265 ***What are the time-variant characteristics of stream water age of urban and non-urban streams?***

12  
13  
14 266 The integrated flow-tracer model gave an estimate of the age distribution of streams draining  
15  
16 267 catchments with differential levels of urbanisation. Unsurprisingly, this infers a much higher  
17  
18 268 proportion of newer water, and less tailing of older water, than shown in time-invariant TTD analysis  
19  
20 269 (see Table 4 and Soulsby et al., 2014). It is striking just how much of the precipitation in urban-  
21  
22 270 impacted areas appears to reach the stream within a few days, given the implications for storage  
23  
24 271 and low flows. However, this also reflects the model structure that simply assumed rapid runoff  
25  
26 272 from the urban areas, rather than for example, deeper infiltration in gardens etc. in order to  
27  
28 273 maintain minimal parameterisation (Kirchner, 2006). It is clear that our model does not attempt to  
29  
30 274 accommodate the hydraulic infrastructure of the complex reality in urban systems. However, in the  
31  
32 275 absence of more spatially distributed and higher temporal resolution (sub-daily) flow and tracer data  
33  
34 276 to conceptualize and evaluate a more complex model, such efforts would likely result in increased  
35  
36 277 uncertainty (Beven, 2012). Although we did not present formal uncertainty analysis, the posterior  
37  
38 278 variability of the best 500 parameter sets retained after multi-objective optimization provides an  
39  
40 279 uncertainty proxy; Andrews et al. (2011) showed that the best parameter sets using such  
41  
42 280 optimization methods falls into the range of behavioural parameter sets defined using more formal  
43  
44 281 uncertainty analysis. Also, the model was internally constrained using isotope time series from three  
45  
46 282 sub-catchments resulting in generally good tracer simulations over 2.5 years of marked  
47  
48 283 hydroclimatic variability (Fig. 4) with mostly identifiable parameters (Fig. 5) (Birkel et al., 2014). As a  
49  
50 284 result the isotope simulations for the three sub-catchment time series outperformed flow  
51  
52 285 simulations (Table 3).  
53  
54  
55  
56  
57  
58  
59  
60

286

287 Damped tracer signals increase uncertainty of simulations in the rural catchment (MTT = 473 days  
288 with a 95<sup>th</sup> percentile range of 326 - 864 days; Table 4). A bimodal distribution was simulated with  
289 relatively young waters being derived from the upper soil reservoir in wet periods, consistent with  
290 agricultural drainage effects in the low-lying areas. However, a greater proportion of older water  
291 draining by slower flow paths gives bimodality in age distributions at about 1 year and heavier tailing  
292 beyond this. Such complex age distributions derived from conceptual models using flux tracking  
293 have also been reported by Dunn et al. (2010) and Hrachowitz et al. (2013). Notwithstanding the  
294 influence of hydroclimatic variability on stream water age, the bi-modal distributions are more  
295 consistent with differences in land use and the resulting variability in flow pathways. Such effects of  
296 variable flow pathways on TTDs was also shown by Heidbuechel et al. (2013) albeit in a more  
297 markedly seasonal semi-arid catchment in Arizona, USA. Mixing assumptions also influences time-  
298 variable TTDs (van der Velde et al., 2014) and the complete mixing used here is overly simplistic.  
299 However, the combination of three parallel reservoirs with one nonlinear parameterization creates a  
300 more dynamic catchment scale conceptualisation for assessing the time-variant TTDs.

301

302 The characterisation of TTDs achieved with the integrated flow-tracer modelling approach is an  
303 improvement on using an invariant convolution integral model (Table 4). Although these showed the  
304 same ranking of MTTs (e.g. urban site < outlet site < rural site), the resulting MTTs are longer than  
305 those produced by the time-variant modelling by a factor of 2.1 for urban, 2.4 for rural and 1.62 for  
306 the outlet showing the instability of the time invariant GM for short (<5 year) data time series  
307 (Hrachowitz et al., 2009). Nevertheless, for both the urban and outlet sites, GM estimates fall within  
308 the 95<sup>th</sup>ile error bands of the flow-tracer model.

309

1  
2  
3 310 ***How is time variant streamwater age affected by integration of different land use at larger scales?***

4  
5 311 Time variant flow-tracer modelling allowed us to develop a hypothesis of catchment function which  
6  
7 312 integrates the urban impact on stream water ages at different scales. This is based on the  
8  
9 313 integration of sub-catchments and their dominant processes in relation to land use, which can be  
10  
11 314 seen as upscaling runoff generation and solute transport processes from the hillslope (e.g. Tetzlaff et  
12  
13 315 al., 2014) to catchment scale. Use of multi-objective calibration targets produced a reasonable  
14  
15 316 representation of the runoff and isotope response in the two main sub-catchments and at the  
16  
17 317 catchment outlet (Fig. 4). The isotope damping at the rural site leads to larger uncertainties, in the  
18  
19 318 summer tracer simulations, and this propagates to the outlet site. Despite this, for most of the study  
20  
21 319 period, simulations capture the dynamic influence of the two headwater tributaries isotopes at the  
22  
23 320 outlet. Thus, the strong influence of the short-term dynamic of urban drainage is evident in the  
24  
25 321 modal age class of 50-100 days at the outlet site, but the bimodality shows the greater volumetric  
26  
27 322 contributions of older water from the rural catchment in the secondary peak at 300 days (Fig. 6d). It  
28  
29 323 is also notable that despite the similar percentage urban cover at the urban and outlet sites, the  
30  
31 324 effect is much greater at the former, though the urban impact remains cumulative at the outlet.

32  
33  
34  
35  
36 325

37  
38  
39 326 Although these contrasts mainly reflect the moderating effect of the rural catchment at higher flows,  
40  
41 327 they may also reflect differences in the catchment land use and the nature of the urban  
42  
43 328 developments. The non-urban areas in the sub-catchment of the urban site are predominantly (59%)  
44  
45 329 rough grazing, whilst in the sub-catchment of the rural site it is mainly (64%) forest. This is likely to  
46  
47 330 result in longer residence times in the forested areas due to lower artificial drainage and greater  
48  
49 331 infiltration to depth (e.g. Geris et al., 2014). In addition, urban areas in the upper catchment above  
50  
51 332 the urban site are mainly housing up to 15 years old, which has a higher density of impermeable  
52  
53 333 surfaces and limited sustainable urban drainage systems (soakaways, retention wetlands etc). In  
54  
55 334 contrast, urbanisation in the lower catchment is more recent (mostly <10 years), on-going and  
56  
57  
58  
59  
60

1  
2  
3 335 comprises an industrial estate and retail outlets, with less dense coverage of impermeable surfaces,  
4  
5 336 more green space, permeable parking areas and some retention ponds (cf. O'Driscoll et al., 2010).  
6  
7 337 Lower density urban development is likely to increase water age due to greater sub-surface storage  
8  
9 338 and mixing (and therefore decrease impacts), but modelling this would require explicit integration of  
10  
11 339 more detailed land use classes accompanied by corresponding data for parameterization. Such  
12  
13 340 improvements to the current model are under way and future work will be directed at detailed  
14  
15 341 investigations about the impacts of smaller scale urbanisation of variable density on stream water  
16  
17 342 ages (cf. Thompson et al., 2013).  
18  
19  
20  
21 343

22  
23  
24 344 ***Can we project the impact of increased urbanisation on the composition of stream water age?***

25  
26  
27 345 The flow-tracer modelling approach already shows promise as a tool for predicting change in TTDs  
28  
29 346 resulting from further urbanisation, with the increasing dominance of younger waters at both the  
30  
31 347 urban and outlet sites likely to result from the urban growth already planned in the catchment (Fig.  
32  
33 348 7). However, as noted, the approach is simplistic and work is needed to reduce the inherent  
34  
35 349 uncertainties and provide knowledge transfer for urban design. A key need is higher resolution data  
36  
37 350 (Kirchner et al., 2004); modelling at a daily time step is only a first approximation in assessing urban  
38  
39 351 effects on TTDs. Although sampling targeted high flow events, in reality, the response time of  
40  
41 352 impermeable urban surfaces is much less than this and will influence stream flows on a sub-hourly  
42  
43 353 basis during more intense precipitation (O'Driscoll et al., 2010). Thus, collecting high resolution data  
44  
45 354 to refine the model for sub-daily scales is needed to characterise the faster tail of the TTD and its  
46  
47 355 overall influence more realistically (Birkel et al., 2012). The current uncertainties are reflected in the  
48  
49 356 95<sup>th</sup> percentiles around the MTTs calculated from the best 500 parameter sets (Table 3). At the  
50  
51 357 outlet this results in a MTT of 280 days with 95<sup>th</sup> percentiles of 208 to 520 days. Although these  
52  
53 358 ranges imply some overlap in the CDFs, the general features such as the observed bi-modality and  
54  
55 359 the direction of projections from rural to more urban remain unaffected.  
56  
57  
58  
59  
60



1  
2  
3 360  
4  
5

6 361 In addition, dynamics of the longer residence time waters need to be constrained by (a) using tracers  
7  
8 362 that can quantify ages beyond the 5 year limit of stable isotopes (Stewart et al., 2010) and (b)  
9  
10 363 tracking the catchment response over longer periods (Hrachowitz et al., 2009). Despite constraining  
11  
12 364 the older waters in the flux tracking approach by looping the observed time series, it is unlikely that  
13  
14 365 all potential climatic variability is captured over relatively short monitoring periods, though the 2.5  
15  
16 366 years used here were remarkably variable. This is illustrated by previous analysis of the data from  
17  
18 367 the study site in the first year which covered a relatively dry period: the characterisation of TTDs for  
19  
20 368 the urban and outlet sites in this case showed they were relatively similar (see Soulsby et al., 2014).  
21  
22 369 The new analysis presented here using the 2.5 year data set, including two wetter periods and a  
23  
24 370 more pronounced summer dry period (Figure 2) than were observed in the first year, showed much  
25  
26 371 larger water age differences than previously reported.  
27  
28  
29

30 372  
31  
32

33 373 Finally, the model calibration resulted in substantial uncertainties stemming from the lack of  
34  
35 374 distributed continuous flow data, particularly from the rural tributaries and the integration of  
36  
37 375 temporally different flow contributions from tributaries to the catchment outlet. Whilst this does  
38  
39 376 not affect the general conclusions derived from daily time steps, it would be inadequate for  
40  
41 377 assessing the sub-daily variations described above. Future work will focus on improving monitoring  
42  
43 378 which in turn can be used to develop a more complex and spatially explicit model. We therefore  
44  
45 379 envision incorporating wetlands and soakaway systems as temporary stores, and a lower reservoir in  
46  
47 380 the urban store that allows infiltration to deeper flow paths, sewer overflow and drainage exports.  
48  
49

50 381  
51  
52

53  
54 382 The model's capability in integrating intra-catchment differences in daily flow and isotope responses  
55  
56 383 to better understand the heterogeneity of processes that underpins catchment water age  
57  
58  
59  
60

1  
2  
3 384 distributions is encouraging. There is clear potential use of such insights in urban planning for a  
4  
5 385 sustainable water environment. If the data limitations outlined above can be overcome, an evidence  
6  
7 386 base would emerge that potentially could provide specific guidance on the timescale of water fluxes  
8  
9 387 that could be targets for water retention in new urban developments. This could include, for  
10  
11 388 example, guidance on the design of green infrastructure such as wetlands and detention ponds or  
12  
13 389 permeable surfaces to maintain storage to mitigate flood risk, sustain low flows and improve highly  
14  
15 390 relevant water quality. Currently, such infrastructure is developed from guidelines that often have  
16  
17 391 little specific context for the hydrology and landscape for where the development is occurring.  
18  
19 392 Similarly, as urban development often occurs in a piecemeal *ad hoc* way, the scaling of impacts and  
20  
21 393 their cumulative effects are often ignored. Whilst such issues remain substantial challenges, we  
22  
23 394 present a first step to better understand the cumulative impact of urbanisation on transit times that  
24  
25 395 could be used in future to create more sustainable approaches to urban water management.  
26  
27  
28  
29  
30  
31

396

## 397 **6. Conclusion**

398 Flux tracking is a useful tool for characterising complex time-variant water age distributions and their  
399 spatial aggregation in catchments impacted by urbanisation. Whereas previous studies have usually  
400 looked at input-output relationships for individual catchments (Hrachowitz et al., 2013) or different  
401 hydrological response units within a catchment (Birkel et al., 2014), here we have shown its utility in  
402 integrating responses from contrasting units in a mixed land cover catchment. The dramatic impact  
403 on urbanisation on the quick responding part of the TTD is captured both at the local and larger  
404 catchment scale. The flow-tracer model captured bi-modal TTDs with a higher proportion of young  
405 water and less tailing of older water than using time-invariant models. Though challenges remain,  
406 the approach provides a step towards a framework that could be used in urban design that seeks to  
407 restrict the rapid water fluxes traditionally associated with urbanisation and maintain catchment  
408 storage to sustain low flows, mitigate flood risk and ameliorate water quality impacts.

1  
2  
3 409  
4

5 410 **Acknowledgements**  
6

7 411 The help of Clara F. Soulsby with the sampling is gratefully acknowledged.  
8

9 412  
10  
11  
12  
13  
14  
15  
16  
17  
18  
19  
20  
21  
22  
23  
24  
25  
26  
27  
28  
29  
30  
31  
32  
33  
34  
35  
36  
37  
38  
39  
40  
41  
42  
43  
44  
45  
46  
47  
48  
49  
50  
51  
52  
53  
54  
55  
56  
57  
58  
59  
60

For Peer Review

413 **References**

414 <http://aberdeenshire.gov.uk/statistics/area/BanchoryProfile2013.pdf>

415

416 Andrews F, Croke B, Jakeman A. 2011. An open software environment for hydrological model  
417 assessment and development. *Environmental Modelling & Software* **26**: 1171–1185,  
418 doi:10.1016/j.envsoft.2011.04.006.

419

420 Beven K. 2012. *Rainfall-runoff modelling: The Primer*. Second edition. Wiley-Blackwell.

421

422 Birkel C, Soulsby C, Tetzlaff T, Dunn S, Spezia L. 2012. High frequency storm event isotope sampling  
423 reveals time-variant transit time distributions and influence of diurnal cycles. *Hydrol. Processes*  
424 **26(2)**: 308–316, doi:10.1002/hyp.8210.

425

426 Birkel C, Soulsby C, Tetzlaff D. 2014. Developing a consistent process-based conceptualization of  
427 catchment functioning using measurements of internal state variables. *Water Resources Research*.  
428 Doi: 10.1002/2013WR014925.

429

430 Botter G, Bertuzzo E, Rinaldo A. 2011. Catchment residence and travel time distributions: The master  
431 equation. *Geophys. Res. Lett.* **38**: L11403, doi:10.1029/2011GL047666.

432

433 Brooks JR, Barnard HR, Coulombe R, McDonnell JJ. 2010. Ecohydrologic separation of water between  
434 trees and streams in a Mediterranean climate. *Nature Geoscience* **3**: 100–104.  
435 <http://www.nature.com/ngeo/journal/v3/n2/full/ngeo722.html>

436

437 Deb K, Pratap A, Agarwal S, Meyarivan T. 2002. A fast and elitist multi-objective genetic algorithm:  
438 NSGA-II. *IEEE Transaction on Evolutionary Computation* **6(2)**: 181–197.

439

440 Davies J, Beven K, Rodhe A, Nyberg L, Bishop K. 2013. Integrated modelling of flow and residence  
441 times at the catchment scale with multiple interacting pathways. *Water Resour. Res.* **49**: 4738–4750,  
442 doi:10.1002/wrcr.20377.

443

444 Duffy CJ. 2010. Dynamical modeling of concentration–age–discharge in watersheds. *Hydrol.*  
445 *Processes* **24**: 1711–1718, doi:10.1002/hyp.7691.

446

447 Fenicia F, Wrede S, Kavetski D, Pfister L, Hoffmann L, Savenije HHG, McDonnell JJ. Assessing the  
448 impact of mixing assumptions on the estimation of streamwater mean residence time. *Hydrological*  
449 *Processes* **24**: 1730–1741, 2010.

450

451 Gall HE, Park J, Harman CJ, Rao PSC, Jawitz J. 2013. Landscape filtering of hydrologic and  
452 biogeochemical responses in managed landscapes. *Journal of Landscape Ecology* **28**: 651–664.

453

454 Geris J, Tetzlaff D, McDonnell J, Soulsby C. 2014. The relative role of soil type and tree cover on  
455 water storage and transmission in northern headwater catchments. *Hydrol. Process., doi:*  
456 [10.1002/hyp.10289](http://dx.doi.org/10.1002/hyp.10289)

457

458 Grimm NB, Faeth SH, Golubiewski NE, Redman CL, Wu J, Bai X, Briggs JM. 2008. Global change and  
459 the ecology of cities. *Science* **319**: 756–760.

- 1  
2  
3 460  
4 461 Heidbüchel I, Troch PA, Lyon SW, Weiler M. 2012. The master transit time distribution of variable  
5 462 flow systems. *Water Resources Research* **48**: 6, doi:10.1029/2011WR011293.  
6 463  
7 464 Heidbuechel I, Troch PA, Lyon SW. 2013. Separating physical and meteorological controls of variable  
8 465 transit times in zero-order catchments. *Water Resour. Res.* **49**: doi:10.1002/2012WR013149.  
9 466  
10 467 Hornberger G, Spear R. 1981. An approach to the preliminary analysis of environmental systems. *J.*  
11 468 *Environ. Manage.* **12**: 7 – 18.  
12 469  
13 470 Hrachowitz M, Soulsby C, Tetzlaff D, Dawson JJC, Dunn SM, Malcolm IA. 2009. Using long-term data  
14 471 sets to understand transit times in contrasting headwater catchments. *J. Hydrol.* **367**: 237– 248.  
15 472  
16 473 Hrachowitz M, Soulsby C, Tetzlaff D, Malcolm IA, Schoups G. 2010. Gamma distribution models for  
17 474 transit time estimation in catchments: Physical interpretation of parameters and implications for  
18 475 time-variant transit time assessment. *Water Resour. Res.* **46**: W10536, doi:10.1029/2010WR009148.  
19 476  
20  
21  
22 477 Hrachowitz M, Savenije H, Bogaard TA, Tetzlaff D, Soulsby C. 2013. What can flux tracking teach us  
23 478 about water age distribution patterns and their temporal dynamics?, *Hydrology and Earth System*  
24 479 *Sciences* **17**: 533-564. DOI:10.5194/hess-17-533-2013.  
25  
26  
27 480 Kirchner JW, Feng X, Neal C. 2001. Catchment-scale advection and dispersion as a mechanism for  
28 481 fractal scaling in stream tracer concentrations. *J. Hydrol.* **254**: 82–101, doi:10.1016/S0022–  
29 482 1694(01)00487-5.  
30 483  
31  
32 484 Kirchner JW, Feng X, Neal C, Robson AJ. 2004. The fine structure of water-quality dynamics: the  
33 485 (high-frequency) wave of the future. *Hydrol. Process.* **18**: 1353–1359. doi: 10.1002/hyp.5537  
34  
35 486 Kirchner JW. 2006. Getting the right answers for the right reasons: Linking measurements, analyses,  
36 487 and models to advance the science of hydrology. *Water Resour. Res.* **42**: W03S04,  
37 488 doi:10.1029/2005WR004362.  
38 489  
39 490 Kling H, Fuchs M, Paulin M. 2012. Runoff conditions in the upper Danube basin under an ensemble  
40 491 of climate change scenarios. *J. Hydrol.* **424–425**: 264–277. doi:10.1016/j.jhydrol.2012.01.001.  
41  
42 492 Lyon SW, Desilets SLE, Troch PA. 2008. Characterizing the response of a catchment to an extreme  
43 493 rainfall event using hydrometric and isotopic data. *Water Resour. Res.* **44**: W06413,  
44 494 doi:10.1029/2007 WR006259.  
45 495  
46 496 McDonnell JJ., et al. 2010. How old is streamwater? Open questions in catchment transit time  
47 497 conceptualization, modeling and analysis. *Hydrol. Processes* **24**: 1745–1754, doi:10.1002/hyp.7796.  
48 498  
49  
50 499 McDonnell JJ, Beven K. 2014. Debates – The future of hydrological sciences: A (common) path  
51 500 forward? A call to action aimed at understanding velocities, celerities, and residence time  
52 501 distributions of the headwater hydrograph. *Water Resources Research* **50**: 5342–5350. DOI:  
53 502 10.1002/2013WR015141.  
54  
55  
56  
57  
58  
59  
60

- 1  
2  
3 503 McGuire KJ, Weiler M, McDonnell JJ. 2007. Integrating tracer experiments with modeling to assess  
4 504 runoff processes and water transit times. *Adv. Water Resour.* **30**: 824–837,  
5 505 doi:10.1016/j.advwatres.2006.07.004.  
6 506
- 7 507 Mullen K, Ardia D, Gil D, Windover D, Cline J. 2011. DEoptim: An R Package for Global Optimization  
8 508 by Differential Evolution. *Journal of Statistical Software* **40(6)**: 1(26).
- 9  
10 509 Niemczynowicz J. 1999. Urban hydrology and water management—present and future challenges.  
11 510 *Urban Water* **1**: 1 – 14.  
12 511
- 13 512 O’Driscoll M, Clinton S, Jefferson A, Manda A, McMillan S. 2010. Urbanization Effects on Watershed  
14 513 Hydrology and In-Stream Processes in the Southern United States. *Water*, **2 (3)**: 605-648.  
15 514 doi:10.3390/w2030605.  
16 515
- 17 516 Rinaldo A, Beven KJ, E. Bertuzzo E, Nicotina L, Davies J, Fiori A, Russo D, Botter G. 2011. Catchment  
18 517 travel time distributions and water flow in soils. *Water Resour. Res.* **47**: W07537,  
19 518 doi:10.1029/2011WR010478.  
20 519
- 21 520 Roa-Garcia MC, Weiler W. 2010. Integrated response and transit time distributions of watersheds by  
22 521 combining hydrograph separation and long-term transit time modelling. *Hydrol. Earth Syst. Sci.*  
23 522 **14(8)**: 1537–1549, doi:10.5194/hess-14-1537-2010.  
24 523
- 25 524 Rodhe A, Nyberg L, Bishop K. 1996. Transit times for water in a small till catchment from a step shift  
26 525 in oxygen-18 content of the water input. *Water Resources Research* **32**: 3497-3511.
- 27  
28 526 Seibert J, Beven KJ. 2009. Gauging the ungauged basin: how many discharge measurements are  
29 527 needed? *Hydrology and Earth System Sciences* **13**: 883-892. DOI:10.5194/hess-13-883-2009.
- 30  
31 528 Soulsby C, Birkel C, Tetzlaff D. 2014. Assessing urbanization impacts on catchment transit  
32 529 times. *Geophysical Research Letters* **41**: 442–448. DOI:[10.1002/2013GL058716](https://doi.org/10.1002/2013GL058716).
- 33  
34 530 Stahl K, Moore RD, Floyer JA, Asplin MG, McKendry IG. 2006. Comparison of approaches for spatial  
35 531 interpolation of daily air temperature in a large region with complex topography and highly variable  
36 532 station density. *Agricultural and Forest Meteorology* **139**: 224–236. DOI:  
37 533 10.1016/j.agrformet.2006.07.004
- 38  
39 534 Stewart MK, Morgenstern U, McDonnell JJ. 2010. Truncation of stream residence time: How the use  
40 535 of stable isotopes has skewed our concept of streamwater age and origin. *Hydrological Processes* **24**:  
41 536 1646–1659.
- 42  
43 537 Tetzlaff D, Seibert J, McGuire KJ, Laudon H, Burns DA, Dunn SM, Soulsby C. 2009. How does  
44 538 landscape structure influence catchment transit time across different geomorphic provinces? *Hydrol.*  
45 539 *Processes* **23**: 945–953, doi:10.1002/hyp.7240.  
46 540
- 47 541 Tetzlaff D, Birkel C, Dick J, Geris J, Soulsby C. 2014. Storage dynamics in hydrogeological units  
48 542 control hillslope connectivity, runoff generation, and the evolution of catchment transit time  
49 543 distributions. *Water Resour. Res.* **50**: 969–985, doi: [10.1002/2013WR014147](https://doi.org/10.1002/2013WR014147).  
50 544
- 51 545 Thompson SE, Sivapalan M, Harman CJ, Srinivasan V, Hipsey MR, Reed P, Montanari A, Blöschl G.  
52 546 2013. Developing predictive insight into changing water systems: use-inspired hydrologic science for  
53  
54  
55  
56  
57  
58  
59  
60

1  
2  
3 547 the Anthropocene. *Hydrology and Earth System Sciences* **17**: 5013–5039. DOI: 10.5194/hess-17-  
4 548 5013-2013.  
5 549  
6 550 van der Velde Y, Heidbüchel I, Lyon SW, Nyberg L, Rodhe A, Bishop K, Troch PA. 2014. Consequences  
7 551 of mixing assumptions for time-variable travel time distributions. *Hydrological Processes* DOI:  
8 552 [10.1002/hyp.10372](https://doi.org/10.1002/hyp.10372).  
9 553  
10 554 Zipperer WC, Wu J, Pouyat RV, Pickett STA. 2000. The application of ecological principles to urban  
11 555 and urbanizing land use. *Ecol. Appns* **10**: 685 – 688.  
12 556  
13  
14  
15 557  
16  
17  
18  
19  
20  
21  
22  
23  
24  
25  
26  
27  
28  
29  
30  
31  
32  
33  
34  
35  
36  
37  
38  
39  
40  
41  
42  
43  
44  
45  
46  
47  
48  
49  
50  
51  
52  
53  
54  
55  
56  
57  
58  
59  
60

For Peer Review

## 1 TABLES

2 **Table 1:** Physical characteristics of the Burn of Bennie catchment (outlet) and the urban and rural  
 3 sub-catchments.

ID	Area (km <sup>2</sup> )	Topography			Land use		
		Elevation range (m)	Mean Elevation (m)	Mean Slope (°)	Urban (%)	Forest (%)	Agri- culture (%)
Urban a)	0.34	36	90	2.51	63.3	36.7	0
Urban	1.68	55	83	2.26	12.4	28.6	59
Urban b)	0.027	4	64.4	1.08	100	0	0
Rural	4.5	104	90	2.83	1.0	63.8	24.7*
Outlet	7.9	117	86	2.65	13.1	68.5	31.5

10 \*: 10.5% catchment area corresponds to wetland area and landfill site.



29 **Table 2:** Isotope summary statistics for the 2.5 years study period (October 2011 – April 2014).

ID		n	Mean	Min	Max	SD
Precipitation	Un-weighted	544	-54.8	-147.3	-8.4	21.7
	Weighted		-59.9			
Urban a)		150	-54.2	-95.0	-26.6	7.6
Urban b)		150	-53.5	-120.0	-14.7	11.6
Urban		157	-53.2	-78.7	-31.6	6.0
Rural		155	-51.6	-61.8	-40.1	3.6
Outlet		162	-52.6	-75.2	-33.5	5.2

30

31

32

33

34

35

36

37

38

39

40

41

42

43

44

45

46

47

48

49

50

51

52 **Table 3:** Best-fit conceptual model simulations and the posterior parameter and performance  
 53 statistics in terms of the 5<sup>th</sup> and 95<sup>th</sup> percentiles around the median.

Parameter	Initial	Posterior variability			
		Best-fit	Median [5 <sup>th</sup> , 95 <sup>th</sup> ]	Median KGE_Q [5 <sup>th</sup> , 95 <sup>th</sup> ]	Median KGE_D [5 <sup>th</sup> , 95 <sup>th</sup> ]
k	[0, 0.2]	0.03	0.03 [0.007, 0.038]	0.62 [0.6, 0.65]	0.76 [0.58, 0.84]
$\alpha$	[0, 0.9]	0.38	0.39 [0.36, 0.78]		
r	[0, 0.5]	0.1	0.49 [0.05, 0.96]		
b	[0, 0.1]	0.003	0.003 [0.003, 0.08]		
u	[0, 1]	0.31	0.26 [0.008, 0.38]		
MV <sub>up</sub>	[1, 500]	244	245 [160, 265]		
MV <sub>low</sub>	[500, 5000]	507	502 [500, 4531]		

54

55

56

57

58

59

60

61

62

63

64

65

66

67

68

69

70

71

72

73

74 **Table 4:** Best-fit lumped convolution integral model (gamma model GM) is compared to the best-fit  
 75 conceptual model (CM) for simulations at the rural and urban tributaries and the outlet. Also given  
 76 are the water age statistics in days (MTT [5<sup>th</sup>, 95<sup>th</sup>]) around the median.

Model	Best-fit MTT (days)	Urban			Rural			Outlet				
		MTT [5 <sup>th</sup> , 95 <sup>th</sup> ]	Best- fit KGE (-)	Best- fit R <sup>2</sup> (-)	Best- fit MTT (days)	MTT [5 <sup>th</sup> , 95 <sup>th</sup> ]	Best- fit KGE (-)	Best- fit R <sup>2</sup> (-)	Best- fit MTT (days)	MTT [5 <sup>th</sup> , 95 <sup>th</sup> ]	Best- fit KGE (-)	Best- fit R <sup>2</sup> (-)
GM	366	-	0.74	0.76	1150	-	0.71	0.7	456	-	0.74	0.75
CM	163	171 [87, 391]	0.86	0.89	521	473 [326, 864]	0.78	0.8	316	280 [208, 520]	0.83	0.85

77

78

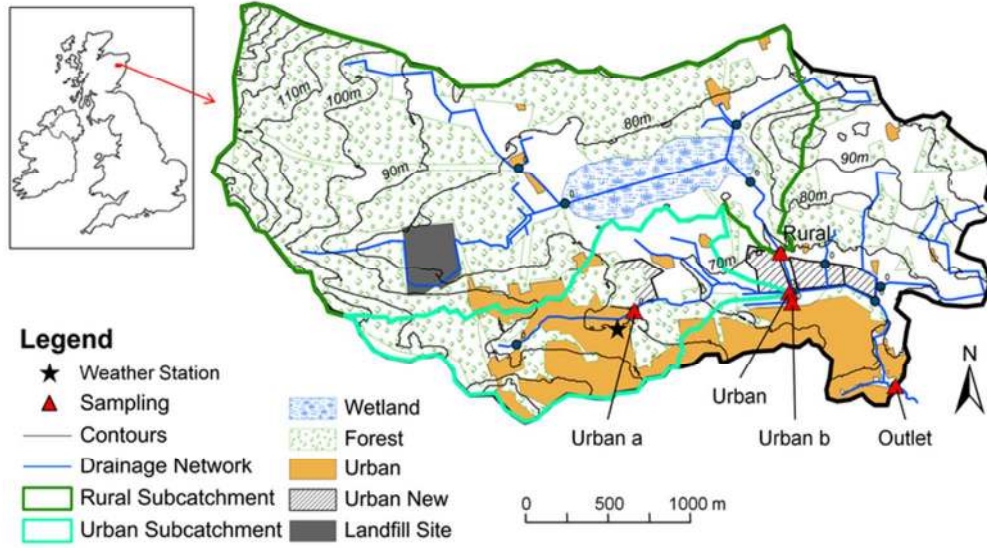


Figure 1: Study catchment location with 5 sampling sites and the main current and proposed extent of land uses (Inset shows location in the UK).  
137x78mm (150 x 150 DPI)

Peer Review

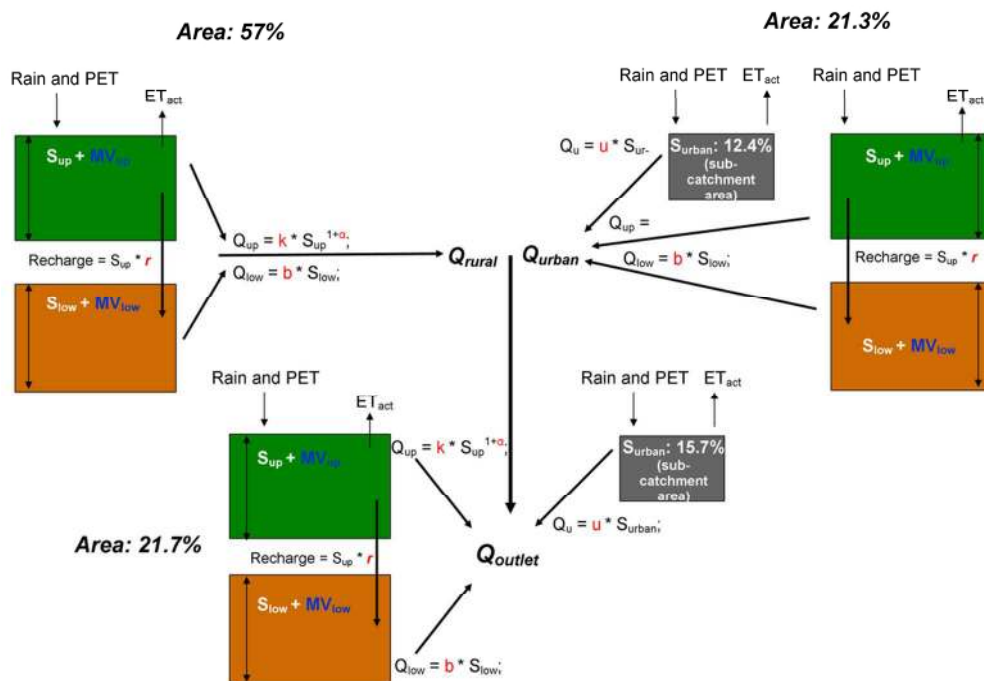


Figure 2: Schematic of model structure and spatial distribution according to catchment configuration. Note that the urban percentages correspond to the respective sub-catchment areas (areas in km<sup>2</sup> given in Table 1), S and MV are dynamic storage and additional mixing volumes, respectively, and that the actual ET effectively equals PET. Flux equations are given with hydrologic parameters in red and the tracer transport is indicated with additional mixing volume parameters in blue. However, the same parameters were used for the different sub-catchments to maintain a minimum of calibrated parameters (in total 7).

197x137mm (150 x 150 DPI)

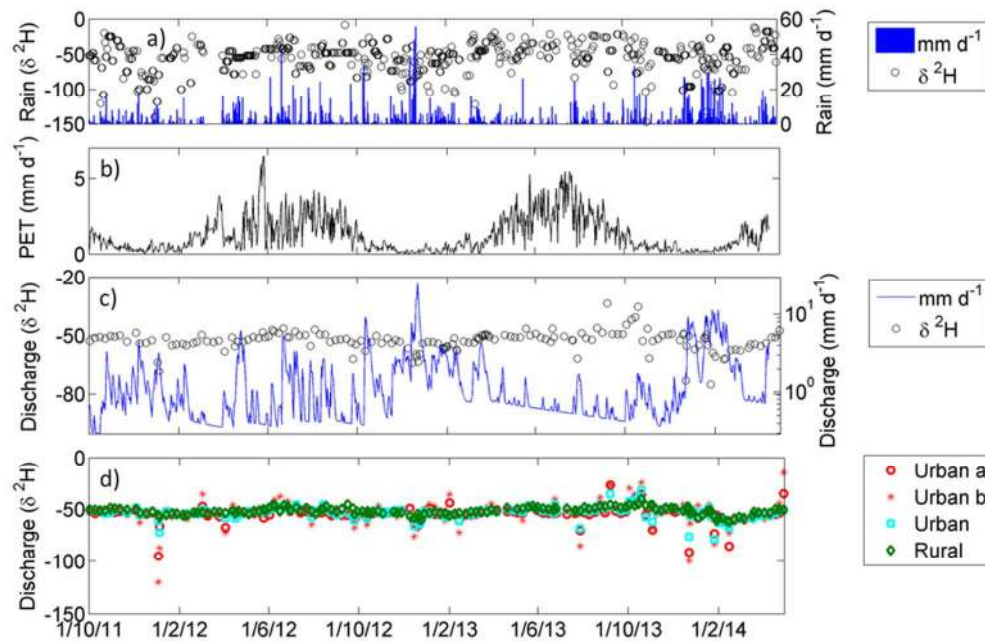


Figure 3: Hydrometric and deuterium isotope daily time series of the study period Oct 2011 to Apr 2014 for a) isotopes and amount of precipitation, b) potential evapotranspiration, c) isotopes and mean simulated discharge at the outlet, and d) discharge isotopes for sites Urban a, Urban b, Urban, and Rural.  
162x104mm (150 x 150 DPI)

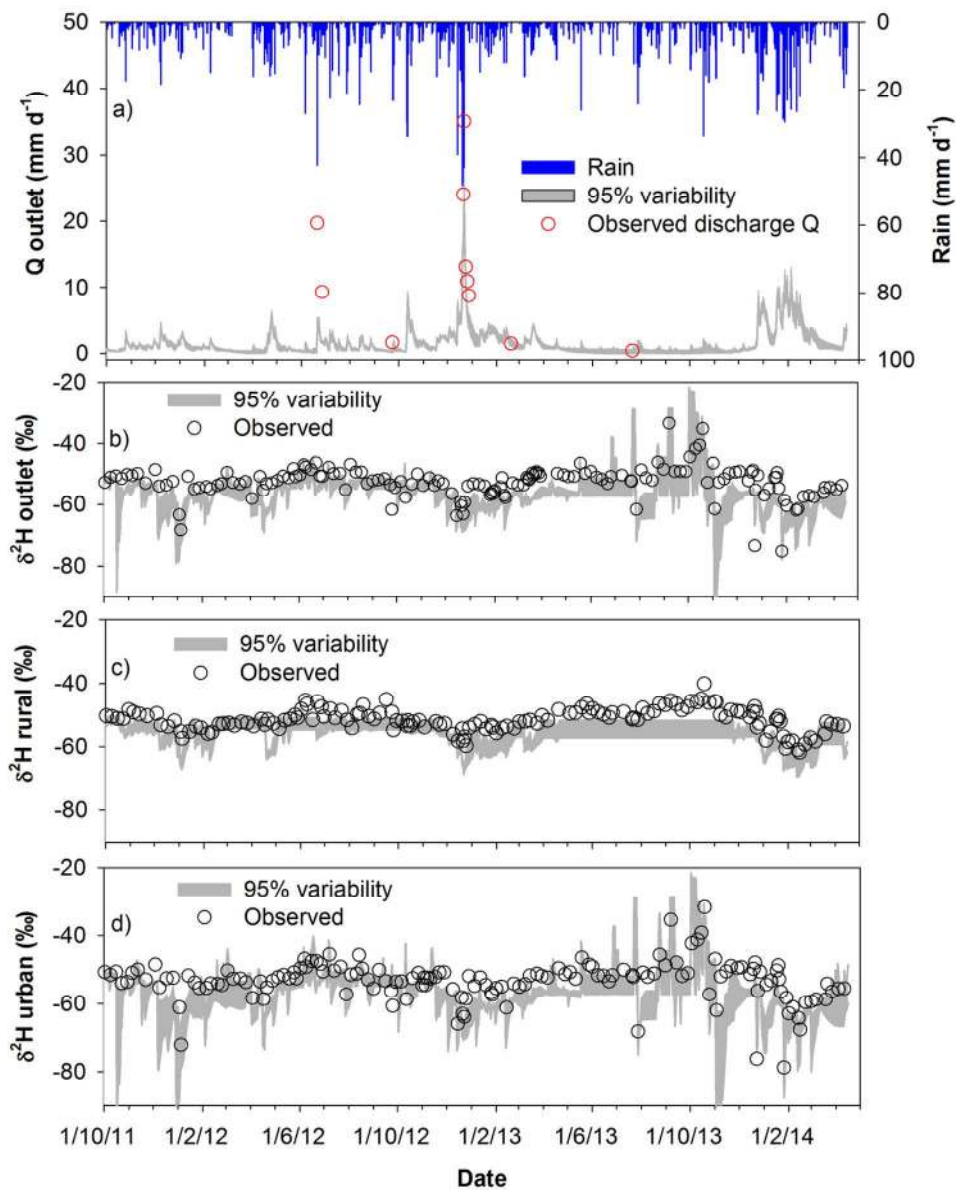


Figure 4: (a) Precipitation and measured and modelled flows at the outlet, together with simulation results showing 95% posterior parameter variability derived from the best 500 parameter sets for the (b) outlet, (c) rural and (d) urban sites.  
254x307mm (150 x 150 DPI)

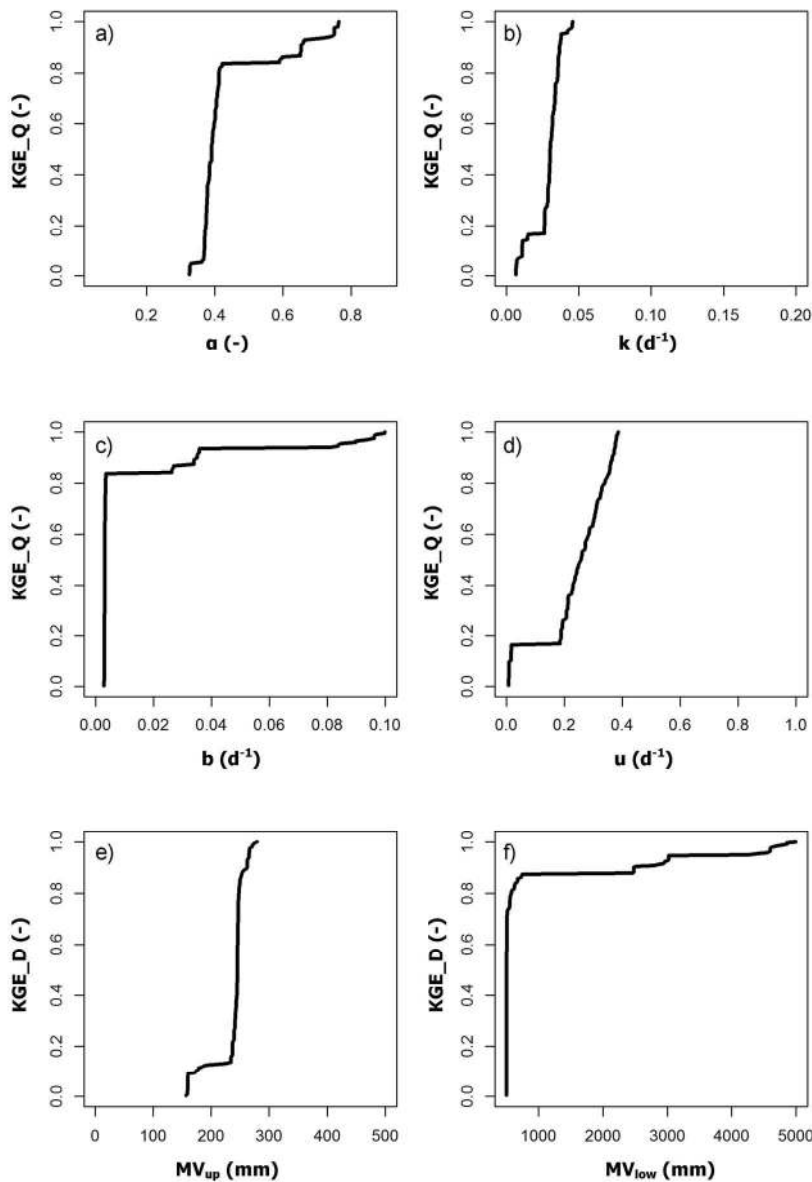


Figure 5: RSA indicates parameter sensitivity for the hydrologic parameters ( $k$ ,  $a$ ,  $b$ , and  $u$ ) evaluated against the discharge calibration target (KGE\_Q) and the tracer parameters ( $MV_{up}$  and  $MV_{low}$ ) against the isotope calibration target (KGE\_D). Increased parameter sensitivity can be derived from stronger curvature compared against a straight line and insensitive parameter. Constrained parameter spaces also indicate parameter sensitivity. Note that the recharge parameter  $r$  is not shown here.  
270x387mm (150 x 150 DPI)



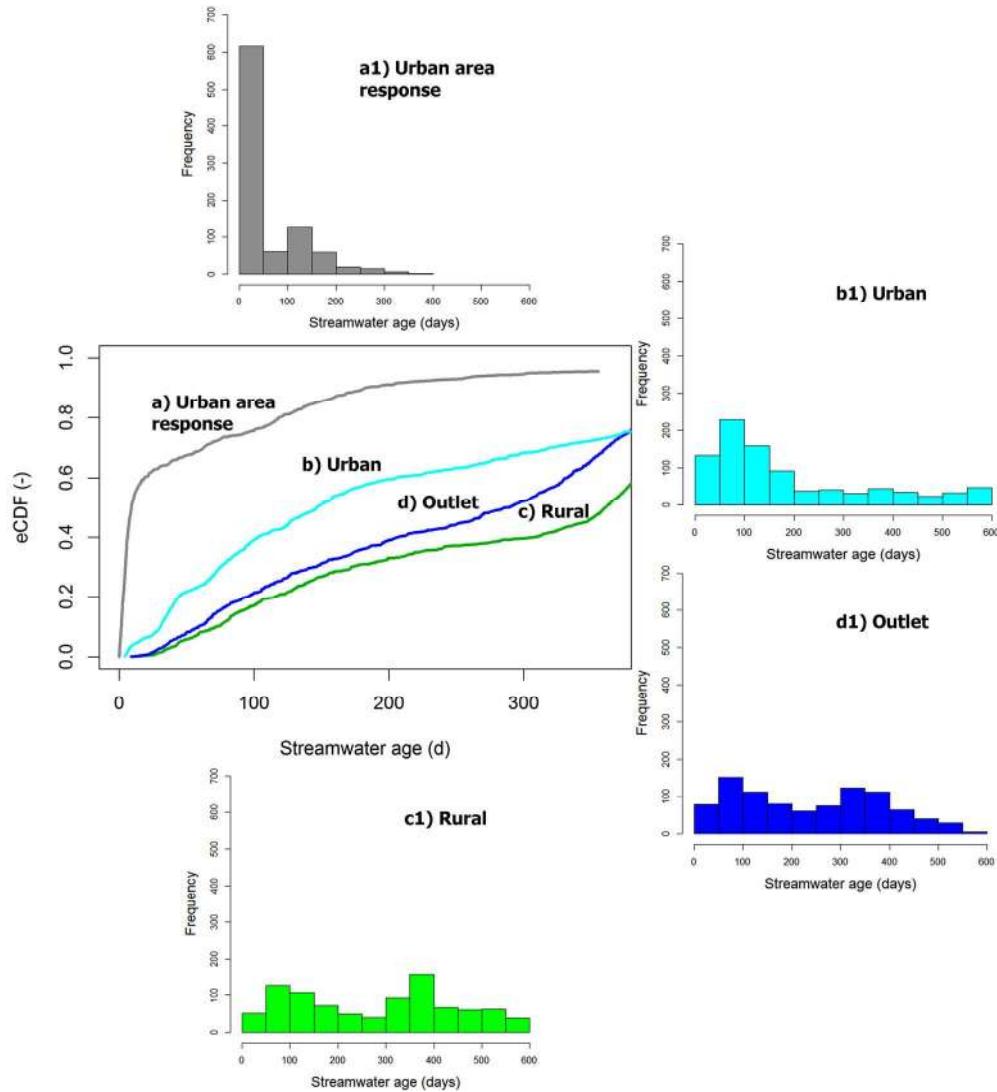


Figure 6: Empirical cumulative median flux water age distribution functions (eCDF) are shown for a) the urban area response (sum of all contributing urban areas), b) the urban and c) rural sub-catchments and d) at the outlet. The streamwater age frequency is visualized as histograms (a1, b1, c1 and d1) using identical axes and classes for comparison.  
342x370mm (150 x 150 DPI)

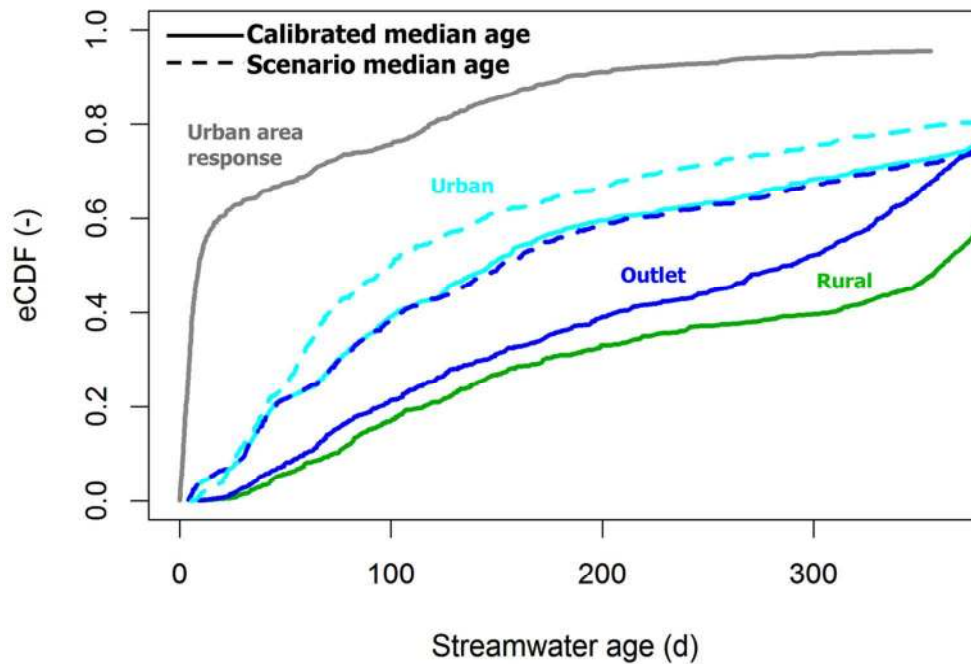


Figure 7: Median water age distributions similar to Figure 6 are compared to scenario water ages (dashed lines) derived from a realistic land use change scenario which will increase the urban cover in the urban sub-catchment and at the outlet by a total of almost 3%. Note that the urban area response refers to the sum of all contributing urban areas.  
225x151mm (150 x 150 DPI)